Chapter 10: Electrochemical Detection of TATA-Binding Protein from a Cell Lysate

This work was performed in collaboration with Jason Slinker, Ali Ebrahim, and Russell Ernst. The multiplexed arrays were fabricated by Jason Slinker.

ABSTRACT

A simple and high-throughput method for the sequence-specific electrochemical detection of TATA-binding protein from complicated mixtures is demonstrated at DNA-modified gold electrodes. The assay is general and based on the interruption of DNA-mediated charge transport to Nile Blue (NB), a redox-active probe covalently attached to the DNA base pair stack. In cell lysate solutions containing nanomolar conentrations of human TBP, we observe a signal attenuation of the NB signal for DNA-modified surfaces containing the TBP binding site; the attenuation is diminished at GC-rich DNA monolayers. Furthermore, in solutions containing murine epithelial cell lysate, we demonstrate the differential detection of upregulated cellular TBP levels with high sequence-specificity. This methodology provides a basis for the sensitive electrical detection of numerous DNA-binding proteins from clinical isolates and on a single DNA chip.

10.1 Introduction

Protein-DNA interactions play a central role in the regulation of nearly all cellular processes including transcription, replication, recombination, and repair. Therefore, the development of sensitive, high-throughput methods to detect the specific binding of proteins to DNA is essential in monitoring pathways for gene expression and in the development of new diagnostics of disease states (1,2). In fact, the examination of gene expression profiles in tumor cells (relative to healthy tissue) can identify "signatures" which forecast the onset of disease and guide the implementation of cancer treatments (3). As such, the reliable detection and identification of properly/improperly functioning DNA binding proteins becomes a crucial area for research and development.

Currently, the most technologically viable methodologies for the detection of protein binding to DNA are based on fluorescence or mass spectrometry. Mass spectrometry, the workhorse of proteomics research, is a harsh technique which degrades the sample during the measurement, making it unsuitable for monitoring delicate, non-covalent protein-DNA interactions (4). By comparison, fluorescent techniques are more gentle and include 1) immunoprecipitation of reversibly crosslinked chromatin/protein complexes (5), 2) capture of fluorescent antibodies by epitope-tagged DNA-binding proteins (6), and 3) amplification of sequences methylated by enzyme/DNA adenine-methyltransferase fusions (7). However, all of these fluorescent methods rely on surface chemistry featuring high lot-to-lot variability and cumbersome optical detection (all within the confines of microbead, microwell, or glass slide formats). In addition, both DNA amplification and extensive labeling of proteins/antibodies are frequently necessary

for fluorescence and mass spectrometry, adding to the expense of these techniques and making them poorly suited for high-throughput assays.

The electrical monitoring of protein/DNA interactions provides a convenient alternative to technologies based on both fluorescence and mass spectrometry (8–13). In fact, a number of recent studies which utilized DNA-functionalized surfaces have demonstrated the feasibility of this approach at small scales (10–13). Within this context, electrochemical assays based on DNA-mediated charge transport (DNA CT) represent a particularly reliable detection strategy for monitoring protein binding at self-assembled DNA monolayers (14-18). Importantly, such assays allow for the interrogation of proteins in their DNA-bound and, therefore, biologically relevant, forms (18).

In a typical electrochemical protein detection experiment, loosely packed DNA monolayers with a covalently appended, electroactive probe are self-assembled in the absence of Mg^{2+}, and the surface is backfilled with an alkanethiol such as mercaptohexanol (9). The resulting DNA films have been characterized extensively with both atomic force microscopy (9, 19) and scanning electrochemical microscopy (20), and the films possess a well-defined morphology with the DNA in an upright orientation, thereby leaving room for proteins to bind. Typically, voltammetry of the DNA-modified electrode is recorded in the absence and presence of protein. Since DNA CT is exquisitely sensitive to perturbation of the base pair stack, detection of protein binding is confirmed by a decrease in the electrochemical yield of charge transfer to a distally-bound probe.

Previously, we have demonstrated the *in vitro* electrical detection of nanomolar concentrations of TATA-binding protein (TBP) not only at DNA-modified macro- and

micro-electrodes (9, 10) but also with scanning electrochemical microscopy (20). TBP is a ubiquitous eukaryotic/prokaryotic protein which plays a central role in the transcriptional machinery as part of the transcription factor IID (TFIID) multi-subunit complex (21–23). Crystal structures of TBP indicate that it resembles a molecular saddle whose concave and hydrophobic underside interacts with the minor groove of DNA, thereby bending the duplex by ~ 90º upon binding (21–23). This unusual binding mode ensures that TBP specifically binds flexible AT-rich tracts, such as its 5'-TATAAAG-3'consensus sequence, and is particularly amenable to detection through attenuation of DNA CT upon binding DNA.

Here we exploit the sensitivity of DNA-modified electrodes for probing protein/DNA interactions to detect the induction of TBP from mouse epithelial cell lysates. Differential expression of TBP is achieved via treatment of epithelial cells with epidermal growth factor (EGF), mimicking the situation encountered in tumorigenesis. By using a multiplexed array which can be independently addressed with DNA featuring a pendant Nile Blue (NB) redox-active probe, we demonstrate the sequence specific detection of the differential expression of TBP. These data underscore the unique technological opportunities presented by electrochemistry at self-assembled DNA monolayers for the reliable detection of DNA-binding proteins.

10.2 Experimental

10.2.1 Materials

All reagents for DNA synthesis were purchased from Glen Research. All reagents for gel electrophoresis were purchased from BioRad, Inc. All antibodies were obtained from AbCam, Inc., and all other reagents for immunoblotting were obtained from Invitrogen, Inc. Mercaptohexanol and buffer preparation reagents were purchased from Sigma in the highest purity available and used as received. Nile Blue perchlorate was purchased from Acros in laser grade purity. Mammalian protein extraction reagent was purchased from Pierce, Inc. Human TATA-binding protein was purchased from Protein One, Inc. Silicon wafers were purchased from Silicon Quest International, Inc. (Santa Clara, CA). Sodium phosphate buffers were prepared with Milli-Q water and pH adjustments were made with sodium hydroxide, if necessary.

10.2.2 Synthesis of Thiol and Nile Blue-Modified DNA

Oligonucleotides were prepared on solid support using standard phosphoramidite chemistry on an Applied Biosystems 394 DNA synthesizer. The pure oligonucleotides were characterized with matrix-assisted laser desorption (MALDI) mass spectrometry, UV-visible (UV-Vis) spectrophotometry, and multiple rounds of high-performance liquid chromatography (HPLC).

Thiol-terminated oligonucleotides were synthesized according to established protocols from Glen Research, Inc., using the C6 S-S thiol modifier. After deprotection and cleavage from solid support with ammonium hydroxide (60 ºC for 8 hours), the disulfide-containing DNA was purified by HPLC. The disulfide was subsequently

reduced with an excess of dithiothreitol in ammonium acetate buffer at pH = 8, and the free thiol containing single-stranded DNA was then purified with a second round of HPLC.

DNA modified with NB at the 5' terminus was prepared according to ultra-mild protocols (Glen Research, Inc.) to avoid degradation of the NB moiety. A 17-mer sequence (5'-UGC GTG CTT TAT ATC TC-3' or 5'-UGC GCG CCC GGC GCC TC-3') was prepared on solid support with a 5-[3-acrylate NHS Ester]-deoxy uridine as the terminal 5' base. The beads were then removed from the synthesizer and dried thoroughly. The solid support were reacted with a 10 mg/mL Nile Blue perchlorate solution in either 9:1 N,N-dimethylformamide/N,N-diisopropylethylamine or 9:1 dichloromethane/N,N-diisopropylethylamine for 12–48 hours. The beads were subsequently washed up to three times with dichloromethane or N,N-dimethylformamide, methanol, and acetonitrile. Subsequently, the Nile Blue-containing sequence was simultaneously cleaved from the support and deprotected with 0.05 M potassium carbonate in methanol at ambient temperature for 12–14 hours. The overall yields of the reaction ranged from 30% to 80%.

Both thiol- and NB-modified DNA was quantified using the extinction coefficient of the single-stranded DNA at 260 nm on a Beckman UV-Vis spectrophotometer. Equimolar amounts of each strand were combined before the resulting solution was purged with argon. Duplexes were formed by thermally annealing to 90 ºC in deoxygenated pH = 7.1 phosphate buffer containing 5 mM NaP_i and 50 mM NaCl, followed by cooling to ambient temperature.

10.2.3 Preparation of Epithelial Cell Lysates

Murine epithelial (JB6) cell lysates were prepared according to the method of Johnson and coworkers (24). In brief, JB6 cells were grown to 80% confluency in 5% fetal bovine serum (FBS) in MEM and then serum deprived using 0.1% FBS in MEM for 3 hours. To induce upregulation of TATA binding protein, cells were then incubated with 50 ng/mL of EGF for 30 to 60 minutes prior to lysis. The cells were washed with phosphate-buffered saline twice and lysed with ~ 1–3 mL of the mammalian protein extraction reagent according to the manufacturer's instructions.

10.2.4 Gel Electrophoresis and Immunoblot Analysis

Denaturing polyacrylamide gel electrophoresis was performed according to established protocols from BioRad. Fresh lysates were loaded onto a denaturing 12% Tris-HCl gel in a 1:1 ratio with Laemmli loading buffer. The gel was electrophoresed for 35 minutes at 200 V using the standard SDS Tris-HCl buffer system.

Western blotting was performed according to established protocols from Invitrogen and AbCam. A freshly electrophoresed gel was transferred to a nitrocellulose membrane via electroblotting for 7 minutes at 30 V with the iBlot gel transfer apparatus available from Invitrogen, Inc. After transfer, the membrane was blocked for 1 hour by incubation in a 5% milk/Tris-buffered saline with Tween solution (TBS-T). The membrane was washed with TBS-T and incubated with an anti-TBP antibody for 1–2 hours at room temperature. After several washes with TBS-T, the membrane was incubated with fluorescein-conjugated goat anti-mouse IgG for 1–2 hours in TBS-T. The membrane was then imaged with a Typhoon 3600 fluorescence imaging system. As a

loading control, the membrane was then blotted with a fluorescein-conjugated anti-β actin antibody for 1–2 hours, washed, and imaged again.

10.2.5 Fabrication of Gold Electrodes

Silicon chips bearing arrays of 16 Au electrodes (.02 cm^2 area each) were fabricated by a two–layer process. In the first layer, the gold electrodes were patterned by a metal lift-off process. The second layer involved patterning Microchem SU-8 photoresist as an insulator to isolate the working areas of the electrodes on the chip surface. Microchem SPR 220 3.0 photoresist was spin-cast at 4000 rpm and baked. The photoresist was patterned with a Karl Suss MA6 contact aligner and a chrome photomask. Following post-exposure baking, wafers were developed in AZ 300 MIF developer and rinsed thoroughly with DI water. A 15 Å Ti adhesion layer and a 1000 Å Au layer were evaporated with a CHA Mark 50 electron beam evaporator. Wafers were then immersed in Microchem 1165 Remover overnight and sonicated as needed to complete lift-off. Subsequently, the wafers were thoroughly baked and cleaned by UV ozone treatment or oxygen plasma etching. Microchem SU-8 2002 was spin cast at 3000 rpm, baked and photopatterned as above. Wafers were developed in Microchem SU-8 Developer and baked for a permanent set of the photoresist. Wafers were diced into 1-inch by 1-inch chips by hand with a diamond scribe.

10.2.6 Preparation of Backfilled DNA Monolayers

Immediately prior to incubation with DNA, gold surfaces were cleaned by sonication in acetone (3 rounds of five minutes each) and isopropanol (1 round of five minutes), followed by treatment with UV-ozone for 3 minutes. Multi-level wells over the electrodes were defined with custom-made viton rubber gaskets and a polypropylene

clamp secured to a test mount. The lower level of the well assembly provided a compression seal that divided the chip into four quadrants of four electrodes near the surface of the chip. This allowed for incubation with up to four distinct sequence of 25–50 μM duplex NB-DNA solution in phosphate storage buffer. Monolayer formation was typically allowed to proceed in a humidified environment for a period of 24–48 hours. Upon completion of film formation, the cell was rinsed thoroughly with phosphate buffer to remove residual DNA before the DNA-modified surface was backfilled with 1.0 mM 1-mercaptohexanol in phosphate storage buffer/5% glycerol for 30–60 minutes. The electrodes and cells were rinsed thoroughly prior to electrochemistry experiments to ensure removal of residual alkanethiols.

10.2.7 Electrochemical Experiments

Cyclic and square wave voltammetry experiments were performed by automated measurement with a CH760B Electrochemical Analyzer and a 16-channel multiplexer module from CH Instruments (Austin, TX). The chips were interfaced with these instruments with a custom built device mount bearing spring-loaded probe pins. Electrochemistry was recorded at ambient temperature in pH 7.1 phosphate buffer containing 5 mM NaP_i, 50 mM NaCl, 4 mM $MgCl_2$, 4 mM spermidine, 50 μM EDTA, 10% glycerol (storage buffer). The custom-manufactured well assembly encompassed all quadrants and electrodes and provided an additional 500 μL of solution capacity. Gold working electrodes in this custom-built cell allowed for experiments with a common Pt auxiliary electrode and a common silver/silver chloride (Ag/AgCl) reference electrode.

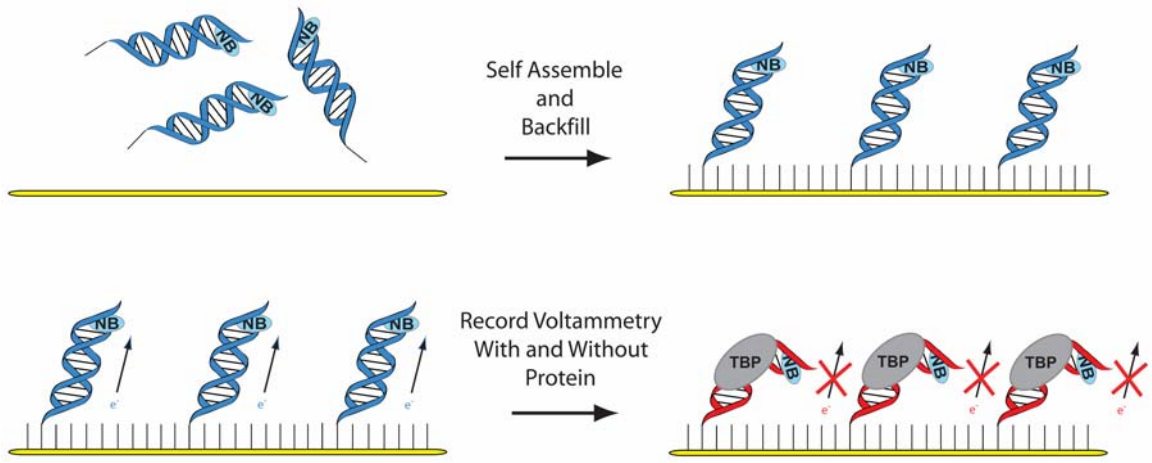

Figure 10.1: Illustration of the self-assembly of DNA monolayers on gold and the subsequent electrochemical analysis of protein binding. First, loosely packed DNA monolayers are formed and the surface is backfilled with mercaptohexanol for passivation. In the absence of TBP, DNA-mediated redox chemistry to the DNA-bound NB is observed. Binding of a protein interrupts the base pair stack and the DNA-mediated redox chemistry, leading to attenuation of the redox signal.

10.3 Results

10.3.1 Experimental Strategy for the Detection of TATA Binding Protein

Figure 10.1 illustrates the strategy for detection of TATA binding protein from cell lysates at DNA monolayers modified with NB-DNA. DNA duplexes containing the 5'-TATAAAG-3' TBP binding site are prepared by hybridizing thiol-modified single-stranded DNA with its NB-modified complement. The duplexes are self-assembled on a clean gold surface in the absence of Mg^{2+} and the surface is backfilled; the resulting monolayer leaves room for the protein to bind. Background voltammetry is recorded initially, and the freshly prepared electrode is subsequently incubated with a small amount of a cell lysate sample before the voltammetry is recorded again. The solution is then supplemented with either human TBP or a lysate sample containing a controlled amount of murine TBP, and the voltammetry is recorded for a third time.

10.3.2 Nile Blue as a Redox Probe for the Detection of Protein Binding

Figure 10.2 shows the cyclic voltammetry (CV) of a DNA monolayer modified at its periphery with NB, which provides a particularly convenient internal standard for the detection of protein binding. DNA monolayers modified with NB display a DNA-mediated redox couple at ~ -200 mV versus Ag/AgCl due to a surface bound species (20). Notably, modification of the exocyclic amine of NB perturbs its aromatic core with an accompanying shift in its redox potential of ~ 200 mV relative to free NB (25, 26). Therefore, DNA monolayer stability can be assessed *in situ*, and the appearance of a NB signal at ~ -400 mV indicates DNA degradation or proteolysis.

A.

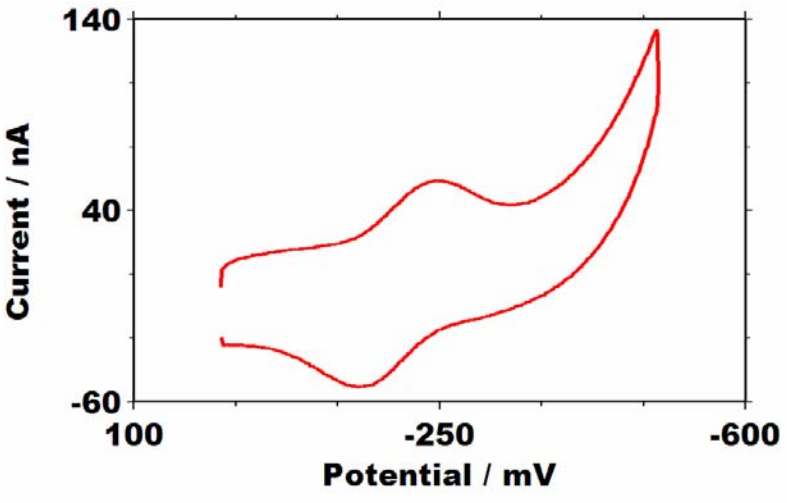

B.

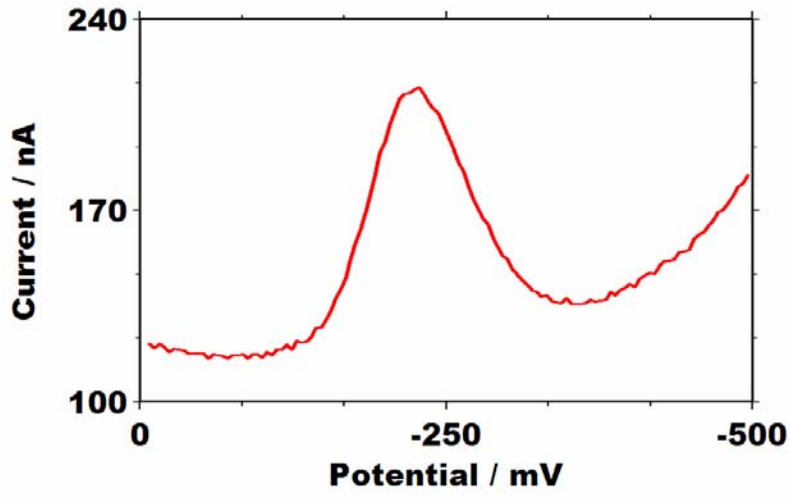

Figure 10.2: CV (A) and SWV (B) of a NB-DNA-modified electrode with a 0.02 cm^2 area at 50 mV/s and 15 Hz, respectively. The electrochemistry buffer is pH=7.1, 5 mM NaP_i, 50 mM NaCl, 4 mM $MgCl_2$, 4 mM spermidine, 50 µM EDTA, and 10% glycerol. The sequence is thiol-5'-GAGATATAAAGCACGCA-3' plus NB-modified complement. Note that the integrated surface coverage found here is ~ 6 pmol/cm^2. The potentials are reported vs. Ag/AgCl.

For somewhat imperfect NB-DNA monolayers, a small signal at ~ -100 mV is observed in addition to the DNA-mediated redox peak at ~ -200 mV. The signal at -100 mV is due to non-specifically bound NB-DNA, as indicated in titration experiments with DNA featuring NB but lacking a thiol (27). This minor side peak provides an additional indicator of film quality prior to protein detection experiments.

The redox couple of NB also serves as an internal standard for changes in buffer conditions due to increased concentrations of lysate. Upon incubation of the electrode with a cell lysate solution, we observe shifts of ~ 20 to ~ 60 mV towards more negative potentials. The pH sensitivity of DNA-bound NB affords a high degree of consistency among different detection experiments and further underscores the attractiveness of NB as an electrochemical probe.

10.3.3 Self Assembly of Nile Blue-DNA Monolayers

Self-assembly of NB-modified DNA monolayers on the gold surfaces of the chips fabricated here is highly reliable and reproducible, as shown in Figure 10.3. In sampling more than 140 electrodes, we find an essentially Gaussian distribution of signal sizes by integration of the cathodic CV peak of NB. The integrated charge ranges from 0 to 6.5 nC with an average value of 4 nC, which corresponds a DNA surface coverage of 1.0 (± 0.4) pmol/cm^2. For comparison, the distribution of signal sizes found for standard rod electrodes cleaned via acid etching and tested under identical conditions is also shown in Figure 10.3. Relative to the freshly deposited gold surfaces, the average DNA coverage drops by a factor of two for rod electrodes (sample size of 14). Surprisingly, although we have observed surface coverages of up to ~ 6 pmol/cm^2 for NB-DNA monolayers (Figure 10.2), our typical coverage falls far short of the coverage of 12 pmol/cm^2 found by

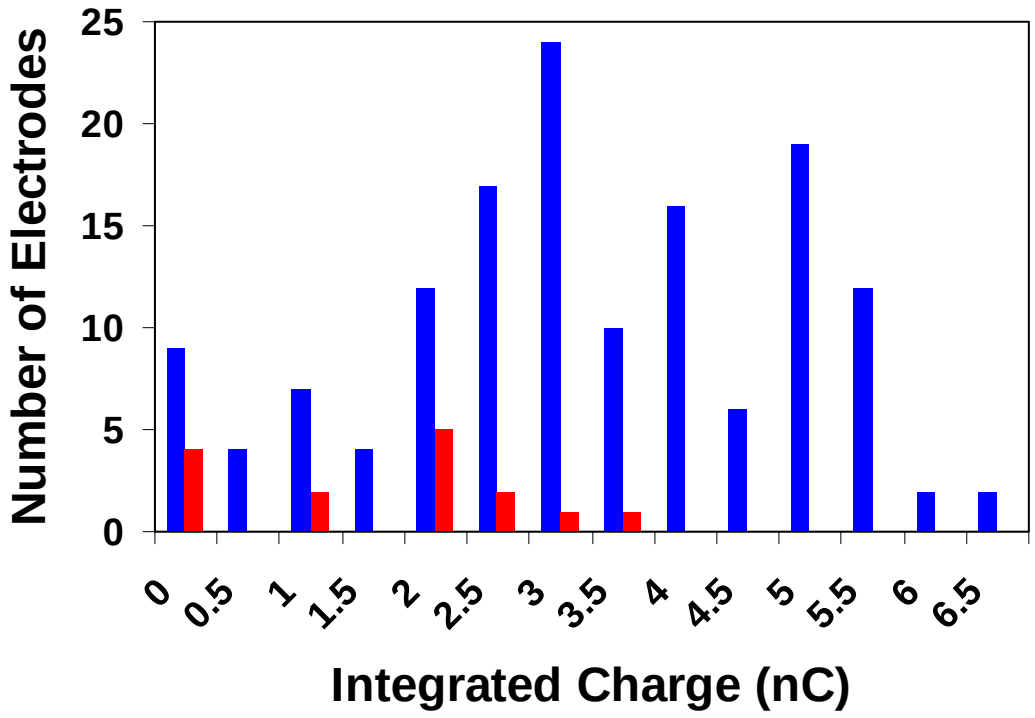

Figure 10.3: An illustration of the distribution of integrated surface charge (cathodic wave) found for NB-DNA monolayers on different gold electrodes prepared under identical conditions. More than 140 electrodes prepared by evaporation of gold on silicon are shown in blue, and 14 electrodes prepared by acid etching of rod electrodes are shown in red. The average value is 4 nC. For ease of comparison, integrated charges have been rounded to the nearest half coulomb. Note that on average a much higher signal and fewer failures are found for gold electrodes fabricated on silicon.

radioactive labeling (9). Nonetheless, the uniform signals obtained here afford excellent statistics which are essential for the proper interpretation of sequence-specific protein detection experiments.

10.3.4 Detection of Human TATA Binding Protein from Cell Lysate Solutions on a Single Substrate

Figure 10.4 shows the effect of a cell lysate on the voltammetry of the NB-modified DNA monolayers on a single chip; a uniform signal loss is observed for films both with and without the TBP binding site. In general, treatment of DNA-modified surfaces with solutions containing high cell lysate concentrations (20% or greater) causes significant initial signal losses which vary from ~ 20 to ~ 50% but are sequence independent. In fact, at lysate concentrations of 20% or greater, a small but significant portion of the DNA films undergoes complete failure. This failure mode is not time dependent and does not typically correlate with DNA degradation; instead, large changes in the background capacitance accompanied are accompanied by complete signal loss. Given that the lysates utilized here were not processed or purified in any fashion, these failures likely result from catastrophic protein adsorption/precipitation onto the electrode surface.

Figure 10.4 also illustrates the effect of 100 nM TBP on DNA monolayers with (TA-DNA) and without (GC-DNA) the TBP binding site in a 20% cell lysate solution and on a single chip. It is important to note that detection experiments with DNA monolayers on a single substrate afford a high degree of reliability and internal consistency. For TA-DNA monolayers featuring the recognition site, the voltammetry of DNA-bound NB is significantly attenuated, but for GC-DNA monolayers missing the

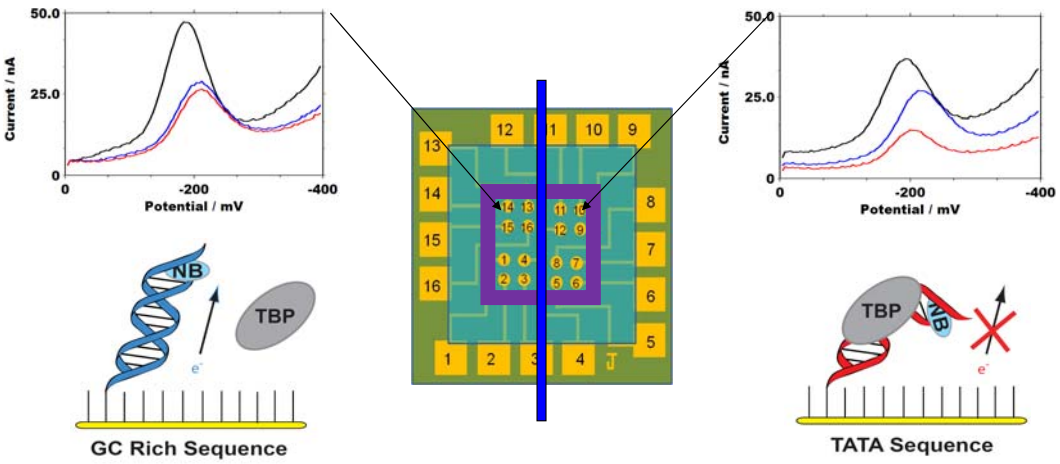

Figure 10.4: SWV of NB-DNA monolayers 15 Hz in dialysis buffer (black), after addition of 20% JB6 cell lysate (blue), and after addition of 100 nM TBP (red). The dialysis buffer is pH=7.1, 5 mM NaP_i, 50 mM NaCl, 4 mM $MgCl_2$, 4 mM spermidine, 50 μM EDTA, and 10% glycerol. The sequence is 5'-UGC GTG CTT TAT ATC TC-3' plus thiol-modified complement (GC rich, left panel) and 5'-UGC GCG CCC GGC GCC TC-3' plus thiol-modified complement in (TA rich, right panel). The DNA-modified electrodes were prepared on the same substrate (center); half of the chip was modified with TA-rich DNA and half of the chip was modified with GC-rich DNA. Note that a greater signal attenuation is observed for the sequence containing the 5'-TATAAAG-3' TBP binding site.

TBP recognition site, the voltammetry is affected to a lesser extent. These observations indicate the sequence-specific recognition of TBP. Upon protein binding, the DNA containing the recognition site is kinked, inhibiting DNA-mediated CT to NB, and a sequence-specific decrease is observed for the NB signal.

10.3.5 Detection of Murine TATA Binding Protein from Whole Cell Lysates

To test the feasibility of our approach for the detection of TATA binding protein produced *in vivo*, detection experiments were also performed with higher lysate concentrations, as schematically illustrated in Figure 10.5. JB6 epithelial cells were treated with epidermal growth factor (EGF) to upregulate TATA binding protein, presumably through activation of the epidermal growth factor receptor (EGFR) (24). The cells were subsequently lysed, and the resulting solution was analyzed electrochemically.

The effect of various cell lysates on TA-DNA and GC-DNA monolayers is summarized in Figure 10.6. To minimize the initial effect of non-specific adsorption, all of the films were initially tested in a 20% JB6 cell lysate solution. Subsequently, the addition of an 80 % by volume solution of EGF-treated epithelial lysate causes a statistically significant signal loss of 63 (±2) % at TA-DNA electrodes (sample size of 15 electrodes), and incubation of GC-DNA electrodes results in a diminished signal loss of 31 (±8) % (sample size of 15 electrodes). By comparison, incubation of TA-DNA- and GC-DNA-modified electrodes with an untreated epithelial lysate does not show a differential effect with signal losses of 18 (±4)% and 17 (±7)%, respectively (sample size of 15 electrodes each). As an additional control, an EGF-treated but heat inactivated cell lysate solution also yields consistent results. For a heat treated lysate, a signal decrease of

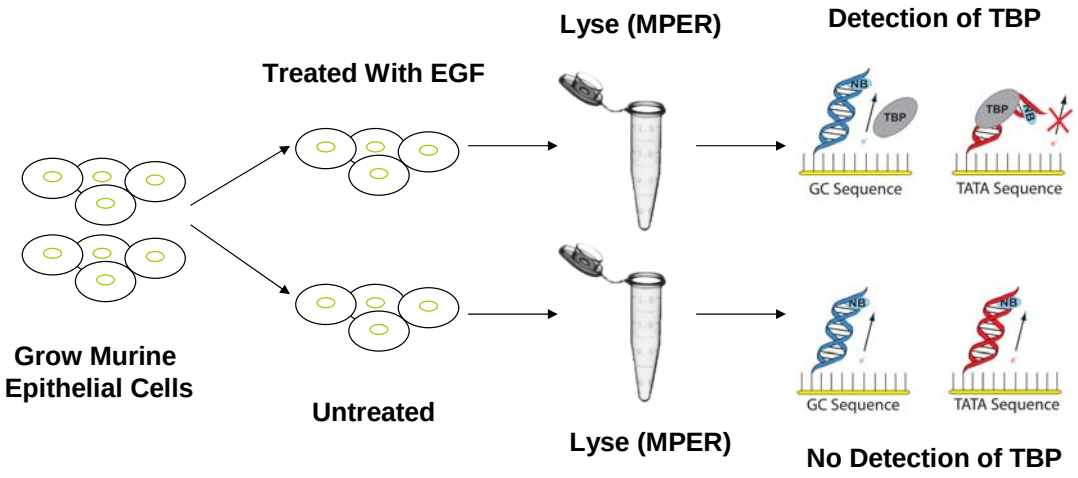

Figure 10.5: A schematic illustration of the growth and lysis of murine epithelial cells. A single batch of cells is split with half of the cells undergoing EGF treatment to upregulate TBP. The cell lysate is subsequently utilized for detection experiments. Sequence specific detection of TBP is achieved only in lysates containing upregulated levels of this transcription factor.

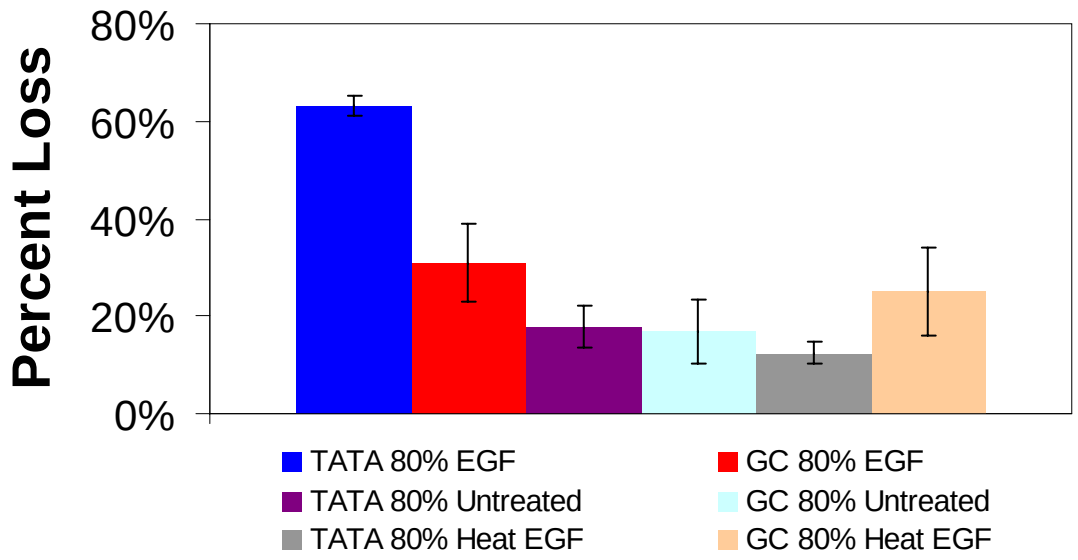

Figure 10.6: A representation of the signal loss found at NB-DNA-modified surfaces after addition of 80% JB6 epithelial cell lysate under various conditions. In each case, the buffer is an 8:2 ratio of cell lysate to pH=7.1, 5 mM NaP_i, 50 mM NaCl, 4 mM $MgCl_2$, 4 mM spermidine, 50 μM EDTA, and 10% glycerol. The sequence is 5'-UGC GTG CTT TAT ATC TC-3' plus thiol-modified complement (blue, purple, and gray) and 5'-UGC GCG CCC GGC GCC TC-3' plus thiol-modified complement in (red, teal, and peach). For the blue and red graphs, overexpression of TBP was induced with EGF. For the purple and teal graphs, overexpression of TBP was not induced. For the gray and peach graphs, overexpression of TBP was induced with EGF but the lysate was heat treated prior to experiments to inactivate TBP. The data was obtained from square wave voltammetry peak currents and represents a minimum of fifteen electrodes (blue, red, purple, teal) or seven electrodes (gray, peach).

25 (±9)% is found for GC-DNA-modified electrodes (sample size of 7), and a signal decrease of 13 (±2)% is found for TA-DNA-modified electrodes (sample size of 7). It is likely that differential effect observed upon heating simply represents the small sample size. Overall, these data strongly indicate the detection of upregulated TBP from a whole cell lysate.

As confirmation of the overexpression of TBP in EGF-treated JB6 epithelial cells, four batches of lysate from independently grown cells underwent Western blotting analysis, as shown in Figure 10.7. The lysates utilized for the majority of the electrochemistry experiments presented above are shown in lanes 3 and 4. As expected, there is a faint band, which corresponds to the human TBP standard in lane 5, for the EGF-treated lysate in lane 4 of the right panel of Figure 10.7. In addition, the TBP band (MW = 42 kDa) is in close proximity to the β-actin loading control (MW = 38 kDa) in the left panel of Figure 10.7. Interestingly, the cells lysates for bands 1 and 2 were treated in an identical fashion to those of lanes 3 and 4, yet the β-actin loading controls indicate lower protein concentrations in lanes 1 and 2, making it difficult to quantify TBP. This indicates that some variation in TBP cellular concentrations is to be expected among lysates.

Analysis of TBP levels by Western blotting also allows us to estimate the concentrations of TBP we are detecting. In untreated cells, if we assume a copy number of ~ 10^5 for TBP (28) and a cell count of ~ 5 million/mL, we obtain an effective TBP concentration of approximately ~ 1 nM, which is similar to the reported binding affinity of TBP (29, 30). The *in vivo* concentration is certain to be higher not only in EGF-treated

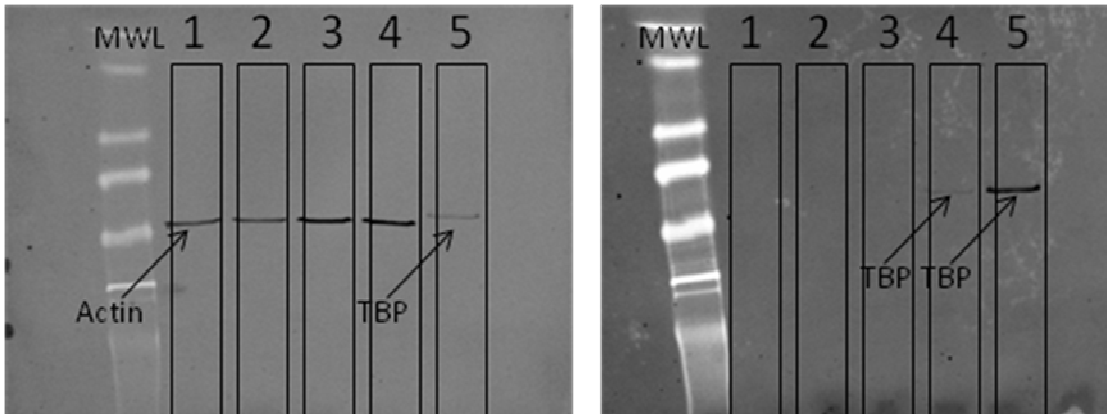

Figure 10.7: Visualization of TBP levels in cell lysates by Western blotting analysis of an SDS-PAGE Tris-HCl gel. A molecular weight ladder is shown for comparison, and a human TBP standard is shown in lane 5. Lanes 1 and 2 correspond to lysate from a single batch of cells, and lanes 3 and 4 correspond to the lysate from another batch of cells. The cells lysed for lanes 2 and 4 were subjected to EGF treatment, while the cells in lanes 1 and 3 were not treated. Note the increased level of TBP in lane 4, and the smaller amounts of actin (relative to lanes 3 and 4) in lanes 1 and 2. The left and right panels are from a single gel, and the black lines are intended as a guide to the eye.

cells but also in more concentrated lysates. Indeed, immunoblotting of TBP standards at various concentrations indicates that the TBP concentrations for the lysates utilized in our experiments may approach the ~ 10 nM range, lending further credence to our observations.

10.4 Implications and Conclusion

We have now demonstrated the electrical detection of TBP binding from a cell lysate at DNA-modified surfaces. In lysate solutions supplemented with human TBP, a dramatic attenuation is observed at DNA-modified surfaces featuring the 5'-TATAAAG-3' consensus sequence, while little attenuation is found for surfaces modified with GC rich DNA. For epithelial cell lysates with upregulated levels of murine TBP, a differential effect of 30% was also observed. Taken together, these data support the assertion of a sequence specific recognition event.

To emphasize the technological feasibility of electrical detection, we can compare the amount of cell lysate required for Western blotting and DNA electrochemistry. Each electrochemical experiment necessitates ~ 10–20 μL of sample per electrode, and each Western blot requires ~ 15 μL of cell lysate per lane. Therefore, the material consumed is comparable in both electrical and fluorescent detection, which is significant given the lower cost of electrical techniques. Through optimization of the electrode size and the electrode housing, it should even be possible to reduce the sample sizes to less than ~ 5 μL per electrode. In addition, some processing of the lysate prior to experiments would also improve on the observed differential detection (relative to background signal losses).

Such experimental challenges are certainly important for electrical detection and warrant further attention in future experiments.

The results presented here are also particularly significant given that TBP plays a central role in the transcriptional machinery and changes in the *in vivo* levels of TBP dramatically influence gene expression. In epithelial cells, increased expression of TBP is triggered by EGFR, and consequently, TBP has been implicated in cellular transformation and oncogenesis (24, 31). Furthermore, higher levels of TBP have even been discovered in human tumors (relative to healthy tissue) indicating that it may play a role in human tumorigenesis (31, 32). Therefore, the development of an electrical strategy for the reliable detection of "native" TBP cellular levels (and by extension the levels of other transcription factors) has implications for the early detection of cancer.

Our data generally underscore the utility of DNA-modified electrodes in detection schemes which take advantage of DNA CT. When compared to traditional fluorescence based detection techniques, electrochemical techniques present attractive features such as lower cost, portable equipment, and simplified multiplexing (8). In addition, the methodology outlined here is based upon an interruption of exquisitely sensitive DNA-mediated electrochemistry, so it is applicable for the detection of a variety of proteins that perturb the base pair stack. Therefore, given our ability to rapidly and reliably detect protein binding to DNA from complicated mixtures, the sequence-specific electrical monitoring of numerous DNA binding proteins on a single platform may now be considered.

REFERENCES

(1) Sikder, D., Kodadek, T. (2005) *Curr. Opin. Chem. Biol. 9*, 38–45.

(2) Bulyk, M. L. (2006) *Curr. Opin. Biotechnol. 17*, 422–430.

(3) van't Veer, L. J., Bernards, R. (2008) *Nature 452*, 564–570.

(4) Hanash, S. M., Pitteri, S. J., Faca, V. M. (2008) *Nature 452*, 571–579.

(5) Lee, T. I., Johnstone, S. E., Young, R. A. (2006) *Nat. Protoc. 1*, 729–748.

(6) Bulyk, M. L. (2007) *Adv. Biochem. Engin./Biotechnol. 104*, 65–85.

(7) Vogel, M. J., Peric-Hupkes, D., van Steensel, B. (2007) *Nat. Protoc. 2*, 1467–1478.

(8) Drummond, T. G., Hill, M. G., Barton, J. K. (2003) *Nat. Biotechnol. 21*, 1192–1199.

(9) Boon, E. M., Salas, J. E., Barton, J. K. (2002) *Nat. Biotechnol. 20*, 282–286.

(10) Gorodetsky, A. A., Ebrahim, A., Barton, J. K. (2008) *J. Am. Chem. Soc. 130*, 2924–2925.

(11) Zheng, G., Patosky, F., Cui, Y., Wang, W. U., Lieber, C. M. (2005) *Nat. Biotechnol. 23*, 1294–1301.

(12) Patolsky, F., Zheng, G., Lieber, C. M. (2006) *Nanomedicine 1,* 51–65.

(13) Gore, M. R., Szalai, V. A., Ropp, P. A., Yang, I. V., Silverman, J. S., Thorp, H. H. (2003) *Anal. Chem. 75*, 6586–6592.

(14) Boon, E. M., Livingston, A. L., Chmiel, N. H., David, S. S., Barton, J. K. (2003) *Proc. Natl. Acad. Sci. U.S.A. 100*, 12543–12547.

(15) Boal, A. K., Yavin, E., Lukianova, O. A., O'Shea, V. L., David, S. S., Barton, J. K. (2005) *Biochemistry 44*, 8397–8407.

(16) DeRosa, M. C., Sancar, A., Barton, J. K. (2005) *Proc. Natl. Acad. Sci. U.S.A. 102*, 10788–10792.

(17) Gorodetsky, A. A., Boal, A. K., Barton, J. K. (2006) *J. Am. Chem. Soc. 128*, 12082–12083.

(18) Gorodetsky, A. A., Dietrich, L. E. P., Lee, P. E. Demple, B., Newman, D. K., Barton, J. K. (2008) *Proc. Natl. Acad. Sci. U. S. A. 105*, 3684–3689.

(19) Erts, D., Polyakov, B., Olin, H., Tuite, E. (2003) *J. Phys. Chem. B. 107*, 3591–3597.

(20) Gorodetsky, A. A., Hammond, W., Hill, M. G., Slowinski, K., Barton, J. K. (2008) *Langmuir ASAP.*

(21) Kim, Y., Geiger, J. H., Hahn, S. H., Sigler, P. B. (1993) *Nature 365*, 512–520.

(22) Kim, J. L., Nikolov, D. B., Burley, S. K. (1993) *Nature 365*, 520–527.

(23) Patikoglou, G. A., Kim, J. L., Sun, L., Yang, S.–H., Kodadek, T. K., Burley, S. K. (1999) *Genes Dev. 13*, 3217–3230

(24) Zhong, S; Zhang, C; Johnson, D. L. (2004) *Molec. Cell. Biol*. 2004 *24* 5119–5129.

(25) Schlereth, D. D., Schmidt, H.–L. (1995) *J. Electroanal. Chem. 380*, 117–125.

(26) Sugawara, K., Yamauchi, Y., Hoshi, S., Akatsuka, K., Yamamoto, F., Tanaka, S., Nakamura, H. (1996) *Bioelectrochem. Bioenerg. 41,* 167–172.

(27) Slinker, J., Barton, J. K. Unpublished results.

(28) Kato, K., Makino, Y., Kishimoto, T., Yamauchi, J., Kato, S., Muramatsu, M., Tamura, T. (1994) *Nucleic Acids Res. 22*, 1179–1185.

(29) Coleman, R. A., Taggart, A. K. P., Benjamin, L. R., Pugh, B. F. (1995) *J. Biol. Chem. 270*, 13842–13849.

(30) Gilfillan, S., Stelzer, G., Piaia, E., Hofmann, M. G., Meisterernst, M. (2005) *J. Biol. Chem. 280*, 6222–6230.

(31) Johnson, S. A. S., Dubeau, L., White, R. J., Johnson, D. L. (2003) *Cell Cycle 2*, 442–444.

(32) Johnson, S. A. S., Dubeau, L., Kawalek, M., Dervan, A., Schonthal, A. H., Dang, C. V., Johnson, D. L. (2003) *Mol. Cell. Biol. 23*, 3043–3051.